Journal of Atmospheric and Solar-Terrestrial Physics 175 (2018) 49–55

Contents lists available at ScienceDirect

Journal of Atmospheric and Solar-Terrestrial Physics

journal homepage: www.elsevier.com/locate/jastp

# Sausage oscillations in a plasma cylinder with a surface current

Daye Lim[a], Valery M. Nakariakov[a,b,*], Yong-Jae Moon[a]

[a] School of Space Research, Kyung Hee University, Yongin, 446-701, Gyeonggi, South Korea
[b] Centre for Fusion, Space and Astrophysics, Department of Physics, University of Warwick, CV4 7AL, UK

ARTICLE INFO

*Keywords:*
Oscillations
Corona

ABSTRACT

Linear sausage oscillations of a cylinder embedded in a plasma with an azimuthal magnetic field, created by a current on the surface of the cylinder, are studied. Such a plasma configuration could be applied to modelling flaring loops, and magnetic ropes in coronal mass ejections. The plasma is assumed to be cold everywhere. Dispersion relations demonstrate that the lowest radial harmonic of the sausage mode is in the trapped regime for all values of the parallel wave number. In the long-wavelength limit, phase and group speeds of this mode are equal to the Alfvén speed in the external medium. It makes the oscillation period to be determined by the ratio of the parallel wavelength, e.g. double the length of an oscillating loop, to the external Alfvén speed, allowing for its seismological estimations. The application of the results obtained to the interpretation of long-period (longer than a minute) oscillations of emission intensity detected in solar coronal structures, gives reasonable estimations of the external Alfvén speed. Cutoff values of the parallel wavenumber for higher radial harmonics are determined analytically. Implications of this finding to the observational signatures of fast magnetoacoustic wave trains guided by cylindrical plasma non-uniformities are discussed.

## 1. Introduction

Oscillatory processes in plasma non-uniformities of the solar corona have been intensively studied observationally for about two decades (e.g., see De Moortel and Nakariakov, 2012; Liu and Ofman, 2014, for recent comprehensive reviews), mainly in the context of solar coronal plasma heating and wave-based diagnostics of the coronal plasma, magnetohydrodynamic (MHD) seismology. The main feature of the solar corona that prescribes MHD wave dynamics, and makes it different from, for example, the Earth's magnetosphere, is the fine field-aligned structuring of the plasma, i.e. the existence of coronal plasma loops and plumes in coronal holes (e.g., Nakariakov et al., 2016). The structuring of the density and temperature of the coronal plasma introduces several important effects affecting MHD waves, such as the possibility of guided wave propagation, occurrence of geometrical dispersion, resonant coupling of compressive and incompressive modes, phase mixing of incompressive modes, etc.

The commonly used theoretical model describing MHD oscillations of a field-aligned plasma non-uniformity is based upon the consideration of MHD perturbations of a plasma cylinder (Zajtsev and Stepanov, 1975; Edwin and Roberts, 1983). In this case, the azimuthal symmetry allows one to make a Fourier transform with respect to the azimuthal angle, introducing an integer azimuthal mode number $m$. An important class of the perturbations are the axisymmetric, $m = 0$ oscillations, often called sausage, radial or peristaltic. We need to stress that in this study we use the term “sausage” for the fast magnetoacoustic modes of coronal plasma structures only. In the low-$\beta$ plasma of the coronal active regions sausage oscillations are characterised mainly by alternate axisymmetric flows in the radial direction, and hence produce essential variations of the plasma density and the absolute value of the magnetic field. It makes this mode easily detectable in both thermal and non-thermal emission (Gruszecki et al., 2012; Van Doorsselaere et al., 2016; McLaughlin et al., 2018). Sausage oscillations have been used for the interpretation of 9-s and 15-s quasi-periodic pulsations (QPP) of gyrosynchrotron emission in a flaring loop (Melnikov et al., 2005). QPP with the periods of 0.7 s and 2 s, lasting for about 70 s, detected at 4–7 GHz have been associated with sausage oscillations by Mészárosová et al. (2016). QPP of the microwave, hard X-ray and gamma-ray emission of a single flaring loop, with the period about 40 s has been found to be consistent with a sausage oscillation by Nakariakov et al. (2010). This interpretation is supported by the forward modelling of the observational manifestation of a sausage oscillation in the gyrosynchrotron emission performed by Kuznetsov et al. (2015). One-second quasi-periodic wiggles of microwave zebra patterns during a solar flare (Yu et al., 2013; Kaneda et al., 2018) have also been associated with sausage oscillations on the basis of forward modelling (Yu et al., 2016).

Sausage oscillations are also detected in other bands. For example, Srivastava et al. (2008) observed oscillations in the H$\alpha$ emission from a

* Corresponding author. School of Space Research, Kyung Hee University, Yongin, 446-701, Gyeonggi, South Korea.
*E-mail address:* V.Nakariakov@warwick.ac.uk (V.M. Nakariakov).

https://doi.org/10.1016/j.jastp.2018.04.013
Received 30 March 2018; Received in revised form 24 April 2018; Accepted 25 April 2018
Available online 09 May 2018
1364-6826/ 

cold loop, with periods of several minutes, and have linked it with a co-existing fundamental and second harmonics of the sausage mode of the loop. 30-s oscillations of the intensity and spectral width of an emission line observed in a slender cool fibril were associated with the sausage mode by Gafeira et al. (2017). Hayes et al. (2016) detected a 20-s QPP of the soft X-ray emission in a solar flare, and have interpreted it as a sausage oscillation. Tian et al. (2016) have interpreted a high-quality 25-s oscillation of the intensity and Doppler shift of a coronal UV emission line, and in the intensity of soft X-ray emission, as a sausage oscillation of a hot flare loop.

Confident detection of sausage oscillations of coronal plasma structures allows for its usage as a seismological probe of the physical conditions in and around the oscillating structure (e.g., Nakariakov et al., 2003; Chen et al., 2015b; Guo et al., 2016). MHD seismology by the sausage mode requires a robust understanding of the relationship of the observables, i.e. the oscillation properties, with parameters of the oscillating plasma structure. It stimulated a number of dedicated theoretical studies of sausage oscillations, which addressed different aspects of the problem.

Since the pioneering works of Zajtsev and Stepanov (1975), Edwin and Roberts (1983) and Cally (1986), it is known that for typical coronal active region conditions, in a low-$\beta$ plasma cylinder with a straight field, surrounded by a low-$\beta$ plasma with the field parallel to the internal field and the cylinder's axis, the sausage mode occurs in two regimes. Waves of shorter parallel wavelengths are trapped, i.e. they are evanescent outside the cylinder, experiencing the total internal reflection at its boundary. The phase speed of the sausage mode in this regime is purely real, provided the plasma is considered to be ideal. Waves of longer wavelengths are leaky, i.e. they are radiated to the external medium by the cylinder that acts as a fast magnetoacoustic antenna. In the leaky regime the phase speed is complex, with the imaginary part describing to the energy losses by the fast magnetoacoustic radiation. The trapped and leaky regimes are separated by the cutoff wavelength that is determined by the ratio of the Alfvén speeds inside and outside the cylinder. In the leaky regime sausage oscillations could have a sufficiently high quality factor to be detectable in observations (Nakariakov et al., 2012). The cutoff wavelength depends also on the radial harmonic number of the sausage oscillation, i.e. the number of the zero crossings by the radial displacement inside the cylinder. Higher radial harmonics have shorter cutoff wavelengths.

In the trapped regime, the sausage oscillation period is determined by the parallel wavelength, and the Alfvén speeds inside and outside the cylinder. However, in the leaky regime sausage oscillation period becomes independent of the parallel wavelength, and is determined by the radius of the cylinder (see, e.g., the discussions in Kopylova et al., 2002; Nakariakov et al., 2012). Thus, the cutoff wavelength value that separates the leaky and trapped regime is of interest for seismology. There have been several dedicated studies of the dependence of the cutoff wave number on parameters of the oscillating plasma structure. Numerical modelling performed by Nakariakov et al. (2012) for a cylinder with a smooth perpendicular profile of the fast speed demonstrated that the cutoff wavelength increases with the steepening of the profile. This result was confirmed analytically by Lopin and Nagorny (2014). Chen et al. (2015a) established that the cutoff wavelength depends weakly on fine multi-shell structuring of the cylinder. Likewise, finite-$\beta$ effects modify the dispersive properties of the sausage mode insignificantly (Chen et al., 2016). Lopin and Nagorny (2015) found out that the cutoff wavelength of all lowest radial sausage harmonics tends to infinity for the cylinders with very smooth profiles of the fast speed, i.e. for those which correspond to the infinite mass of the plasma in the radial cross-section.

In addition, the cutoff value is significantly affected by the magnetic field geometry, i.e. by electric currents. In the compressible case typical for the corona this effect has been addressed in a few dedicated studies only, which were usually limited to the case of a weak twist, and the straight external field (e.g., Erdélyi and Fedun, 2007; Giagkiozis et al., 2015, 2016). Khongorova et al. (2012) (hereafter KMR12) studied sausage waves in a plasma cylinder with an azimuthal magnetic field localised in an annulus, surrounded by a plasma with the magnetic field parallel to the axis of the cylinder. The azimuthal field is created by surface currents. Such a plasma configuration is the simplest approximation to a more realistic, but much more challenging analytically plasma equilibrium with a helical field being a smooth function of the radial coordinate. Despite its simplicity, the KMR12 equilibrium accounts for the main feature of the radially non-uniform magnetic field: on the axis of the cylinder the azimuthal field is identically zero, reaching its maximum at a certain distance from the axis. The straight magnetic field near the axis stabilises kink instability.

KMR12 established that in the presence of the azimuthal field annulus, the lowest radial sausage harmonic is trapped for any parallel wavelength, and that for the parallel wavelength tending to infinity, i.e. the long-wavelength limit, the parallel phase speed tends to the value

$$\frac{\omega}{k} = V_{\mathrm{Ae}}\left[\frac{\log(a_{\mathrm{out}}/a)}{2+\log(a_{\mathrm{out}}/a)}\right]^{1/2}, \tag{1}$$

where $V_{\mathrm{Ae}}$ is the Alfvén speed outside the cylinder, and $a$ and $a_{\mathrm{out}}$ are the inner and outer radii of the azimuthal field annulus, respectively. This work has recently been generalised by Bahari (2017) who found out that the modification of the dispersion curves caused by finite-$\beta$ effects are minimal. A similar lack of the finite-$\beta$ effect on sausage oscillations was established by Inglis et al. (2009); Chen et al. (2018) for a plasma non-uniformity with a straight magnetic field.

The aim of this study is to investigate further dispersive properties of sausage oscillations in a cylinder surrounded by an azimuthal magnetic field, addressing the case when the azimuthal field annulus is very large, allowing one to neglect the outer region with the field parallel to the cylinder. In other words, we consider the situation when the azimuthal field annulus has an infinite outer radius. As in KMR12, the azimuthal field in the external medium is created by a surface current at the boundary of the cylinder. Such a configuration could be considered as an approximation that describes a flaring loop embedded in an active region, and could also possibly describe a magnetic flux rope in a coronal mass ejection (CME). In a more general sense, the use of this model would provide us with some insight into the effects of the external magnetic field that is not parallel to the cylinder, on sausage oscillations.

The paper is structured as follows. In Sect. 2 we present the model. Sect. 3 describes the derivation of dispersion relations. In Sect. 4 we give the phase relations between perturbations of different physical quantities in the sausage mode. Finally, discussion and conclusions are provided in Sect. 5.

## 2. Model and governing equations

Following the formalism developed in KMR12, see also (Mikhalyaev, 2005), we consider a plasma cylinder with a straight axial magnetic field surrounded by a purely azimuthal magnetic field created by a surface current. The equilibrium magnetic field and density are given by the expressions

$$\mathbf{B}_0(r) = \begin{cases} B_{0\mathrm{i}}\mathbf{e}_z, & r < a, \\ (B_{0\mathrm{e}}/\alpha r)\mathbf{e}_\phi, & r > a, \end{cases} \tag{2}$$

and

$$\rho_0(r) = \begin{cases} \rho_{0\mathrm{i}}, & r < a, \\ \rho_{0\mathrm{B}}/(\alpha r)^2, & r > a, \end{cases} \tag{3}$$

respectively, where $a$ is the radius of the cylinder, $B_{0\mathrm{i}}$, $B_{0\mathrm{e}}$, $\rho_{0\mathrm{i}}$, $\rho_{0\mathrm{B}}$ and $\alpha$ are constants, and $e_\phi$ and $e_z$ are the unit vectors in the azimuthal and axial directions. Inside the cylinder, the internal Alfvén speed is defined as $V_{\mathrm{Ai}} = B_{0\mathrm{i}}/(\mu_0\rho_{0\mathrm{i}})^{1/2}$. The plasma density drops off the cylinder, which

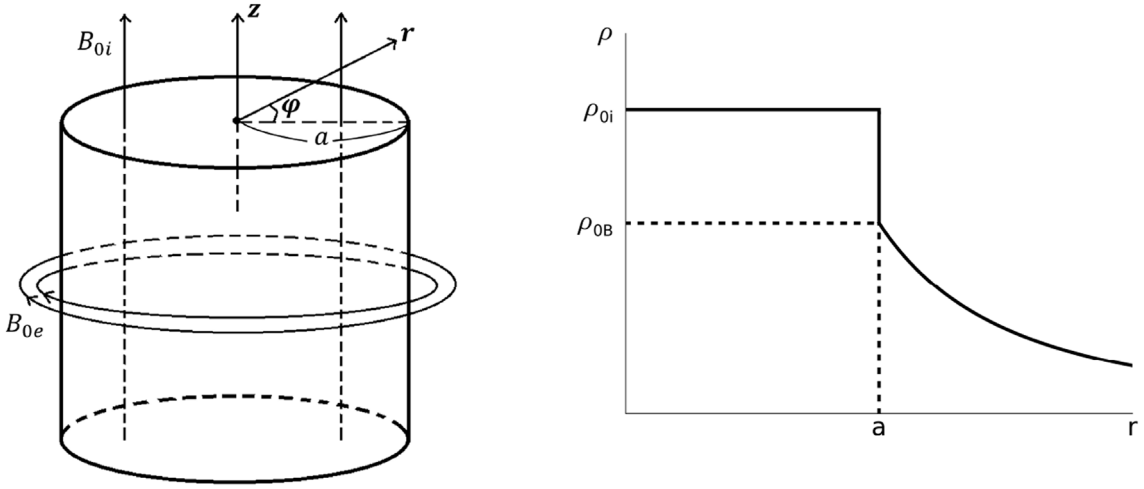


**Fig. 1.** *Left:* Sketch of the magnetic field geometry and the cylindrical coordinate system. *Right:* Radial profile of the plasma density in the equilibrium.

is also consistent with the cases of a coronal loop and CME rope. The combination of the radial dependences of the equilibrium magnetic field and densities in the external medium are chosen to make the external Alfvén speed constant, $V_{Ae} = B_{0e}/(\mu_0\rho_{0B})^{1/2}$. This assumption significantly simplifies the analytical derivation of dispersion relation. In the following, we restrict ourself to the case $\rho_{0i} > \rho_{0B}$, such as $V_{Ai} < V_{Ae}$, which is typical for coronal plasma structures. Thus, the considered model is a simplified version of KMR12, without the external medium with the field parallel to the axis of the cylinder (see Fig. 1). We need to point out that the notations used in this paper are different from those used in KMR12, see, also, Eq. (1).

In this study we consider ideal cold plasmas only. In this case the equilibrium is fulfilled by the magnetic pressure balance at the boundary $r = a$,

$$B_{0i}^2 = \frac{B_{0e}^2}{\alpha^2 a^2}, \tag{4}$$

c.f. condition (2) in KMR12.

The plasma and magnetic field perturbations are described by the linearised MHD equations for an ideal cold (i.e., zero-$\beta$) plasma,

$$\rho = -\rho_0 \nabla\cdot\boldsymbol{\xi} - \boldsymbol{\xi}\cdot\nabla\rho_0, \tag{5}$$

$$\rho_0 \frac{\partial^2 \boldsymbol{\xi}}{\partial t^2} = \frac{1}{\mu_0}(\nabla \times \mathbf{B}) \times \mathbf{B}_0, \tag{6}$$

$$\mathbf{B} = \nabla \times (\boldsymbol{\xi} \times \mathbf{B}_0), \tag{7}$$

where $\mathbf{B}_0 = B_{0\phi}\mathbf{e}_\phi + B_{0z}\mathbf{e}_z$, $\boldsymbol{\xi} = (\xi_r, \xi_\phi, \xi_z)$ is the plasma displacement vector, ρ is the density perturbation, and $\mathbf{B} = (B_r, B_\phi, B_z)$ is the magnetic field perturbation vector (see, e.g., KMR12).

In the following we restrict our attention to the axisymmetric perturbations only, i.e. the derivatives of all quantities with respect to the azimuthal angle are zero. Dependences of the perturbations on the parallel coordinate $z$ and time $t$ are taken proportional to $\exp[i(kz - \omega t)]$, where $\omega$ is the cyclic frequency, and $k$ is the wave number along the axis of the cylinder, called a "parallel wave number". Under those assumptions, the only independent variable is the radial coordinate $r$, in the direction of the plasma and field non-uniformity.

## 3. Dispersion relations

In the internal region $r < a$, equations (5)–(7) reduce to

$$\frac{d^2 P_i}{dr^2} + \frac{1}{r}\frac{dP_i}{dr} + \kappa^2 P_i = 0, \quad \kappa^2 = \frac{\omega^2}{V_{Ai}^2} - k^2, \tag{8}$$

$$\xi_{ri} = \frac{1}{\rho_{0i}(\omega^2 - V_{Ai}^2 k^2)}\frac{dP_i}{dr}, \tag{9}$$

where $P_i$ is the magnetic pressure perturbation inside the cylinder. The solution to (8), which is bounded on the axis ($r = 0$), and corresponds to the body modes ($\kappa^2 > 0$), is given by

$$P_i = A_i J_0(\kappa r), \quad \xi_{ri} = \frac{A_i \kappa J_1(\kappa r)}{\rho_{0i}(V_{Ai}^2 k^2 - \omega^2)}, \tag{10}$$

where $A_i$ is a constant representing the amplitude, and $J_0$ and $J_1$ are the Bessel functions of the zero and first order, respectively. The parameter $\kappa$ is the effective radial wave number of the perturbation inside the cylinder.

In the external region, $r > a$, equations (5) and (6) reduce to

$$\frac{d^2 P_e}{dr^2} + \frac{3}{r}\frac{dP_e}{dr} + \lambda^2 P_e = 0, \quad \lambda^2 = k^2 - \frac{\omega^2}{V_{Ae}^2}, \tag{11}$$

$$\xi_{re} = \frac{\alpha^2 r}{\rho_{0B}\omega^2}\left(r\frac{dP_e}{dr} + 2P_e\right), \tag{12}$$

where $P_e$ is the magnetic pressure perturbation outside of the cylinder. The solution to (11) corresponding to the condition of no energy propagation in the external medium, i.e. the mode trapping condition, is given by

$$P_e = \frac{1}{r}A_e K_1(\lambda r), \quad \xi_{re} = -\frac{\alpha^2 \lambda r}{\rho_{0B}\omega^2}A_e K_0(\lambda r), \tag{13}$$

where $A_e$ is a constant, $K_0$ and $K_1$ are the modified Bessel functions of the second kind, of the zero and first order, respectively. The parameter $1/\lambda$ determines the distance at which the sausage oscillation is localised in the external medium.

Dispersion relations obtained by satisfying the continuity of the radial displacement $\xi_r$ and the total pressure perturbation across the boundary $r = a$, are

$$J_0(\kappa a)K_0(\lambda a) - \frac{J_1(\kappa a)}{\kappa a}\left[K_0(\lambda a) + \frac{\omega^2 a}{\lambda V_{Ae}^2}K_1(\lambda a)\right] = 0. \tag{14}$$

Equation (14) links the frequency and parallel wave number of a sausage perturbation with each other, and also with the parameters of the medium, i.e. with the internal and external Alfvén speeds, $V_{Ai}$ and $V_{Ae}$, respectively, and the radius $a$. The presence of a characteristic spatial scale, the radius of the cylinder, in the problem leads to occurrence of the geometrical dispersion.

Fig. 2 shows dependences of the phase speeds, $\omega/k$, of four lowest radial harmonics, on the parallel wave number, $k$, obtained by numerical solution of algebraic transcendental equation (14). It is evident

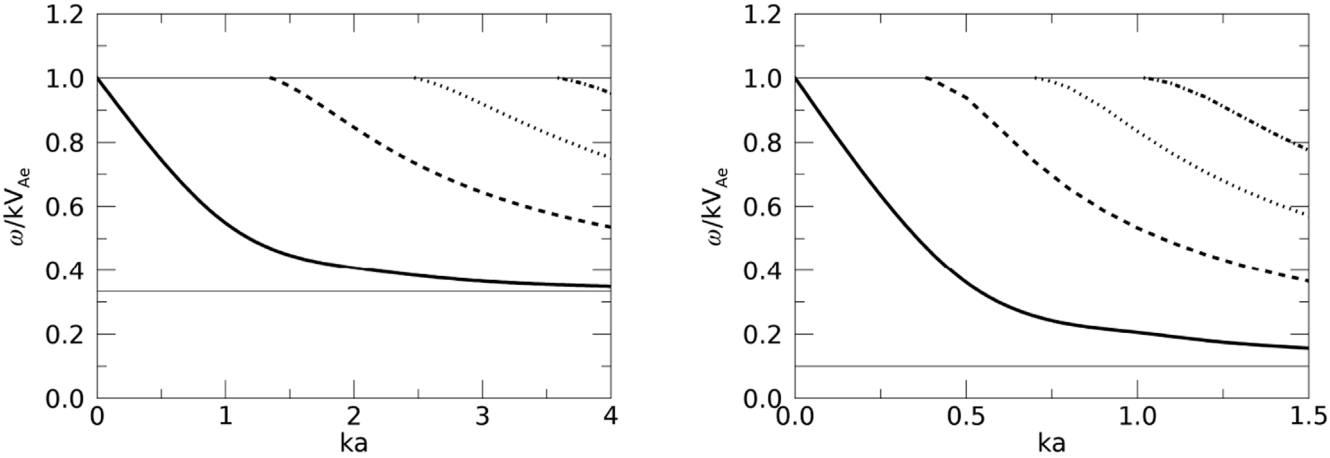


**Fig. 2.** Dependences of the parallel phase speeds of sausage modes on the parallel wavenumber in a plasma cylinder with a surface electric current. The left panel shows the case when the ratio of the external and internal Alfvén speeds is 3, and the right panel of 10. The solid, dashed, dotted, and dash-dotted curves correspond to the first, second, third, and fourth radial harmonics. The upper and lower thin horizontal straight lines show the values of the external and internal Alfvén speeds, respectively. The phase speed is normalised to the Alfvén speed outside the cylinder. The wave number is normalised to the reciprocal of the radius of the cylinder.

that in the considered case the lowest radial harmonic is in the trapped regime for all values of the parallel wave number $k$. In the long wavelength limit, $k \to 0$, the phase speed approaches the external Alfvén speed $V_{\mathrm{Ae}}$. This result could be obtained from equation (1) in the limit $a_{\mathrm{out}} \to \infty$. All other radial harmonics have cutoff wave numbers. At the cutoffs, the phase speed approaches $V_{\mathrm{Ae}}$. Substituting this condition to equation (14) we obtain the cutoff values of the parallel wave numbers,

$$k_{cj} = \frac{V_{\mathrm{Ai}}}{\sqrt{V_{\mathrm{Ae}}^2 - V_{\mathrm{Ai}}^2}}\left(\frac{j_{1n}}{a}\right), \quad n = 0,1,2, \ldots, \tag{15}$$

where $n$ is the radial harmonic number, and $j_{1n} = 0,3.83, 7.02, \ldots$ are the roots of the Bessel function $J_1$. In the short wavelength limit, $k \to \infty$, phase speeds of all radial harmonics approach the internal Alfvén speed. Fig. 3 gives the dependences of the group speeds, $d\,\omega/dk$, along the cylinder. It is evident that the waves of the wavelengths about the radius of the cylinder are highly dispersive. At certain wave numbers the group speeds have minimum values, similarly to the behaviour known in the cylinder surrounded by a plasma with a straight field (e.g. Roberts et al., 1984).

Fig. 4 gives dependences of the radial localisation lengths, i.e. the characteristic radial length of the e-folding of the perturbations in the external medium, of the modes shown in Fig. 2 on the parallel wave number. As in the straight field case (e.g., Edwin and Roberts, 1983), the radial localisation approaches infinity near the cutoff. For smaller wave numbers the phase speed becomes complex, and the wave becomes leaky. We do not consider this regime in this study.

## 4. Phase relations

For the interpretation of observations, and, in particular, for the forward modelling of observables, it is necessary to know the perturbations of different physical quantities. With the use of equations (8)–(10) we obtain the radial structures of the perturbations of the density, absolute value of the magnetic field, and the components of the plasma velocity, respectively,

$$\begin{aligned}
\rho_{\mathrm{i}} &= \tfrac{A_{\mathrm{i}}\kappa^2 J_0(\kappa r)}{\omega^2 - V_{\mathrm{Ai}}^2 k^2}, \\
B_i &= \sqrt{\tfrac{\mu_0^2}{B_{0\mathrm{i}}^2} A_{\mathrm{i}}^2 J_0^2(\kappa r) - \tfrac{k^2 B_{0\mathrm{i}}^2 A_{\mathrm{i}}^2 \kappa^2 J_{\mathrm{i}}^2(\kappa r)}{\rho_{0\mathrm{i}}^2 (V_{\mathrm{Ai}}^2 k^2 - \omega^2)^2}}, \\
v_{\mathrm{ri}} &= -i\omega \tfrac{A_{\mathrm{i}}\kappa J_1(\kappa r)}{\rho_{0\mathrm{i}}(V_{\mathrm{Ai}}^2 k^2 - \omega^2)}, \quad v_{\phi\mathrm{i}} = 0, \quad v_{\mathrm{zi}} = 0.
\end{aligned} \tag{16}$$

Likewise, using equations (11)–(13), we obtain for the external medium,

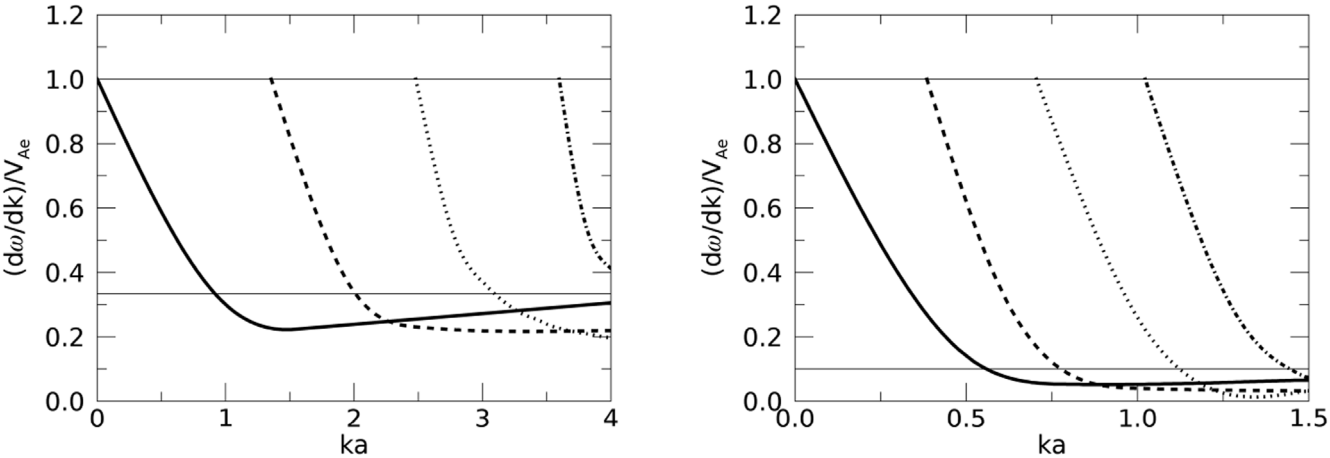


**Fig. 3.** The same as in Fig. 2, but for parallel group speeds.

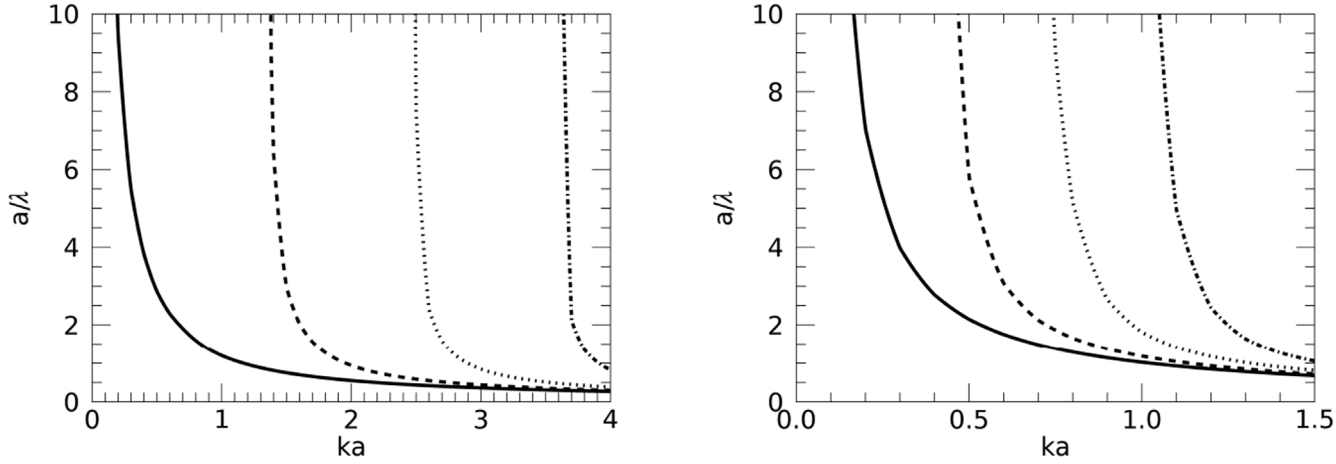


**Fig. 4.** Dependences of radial localisation lengths in the external medium on the parallel wavenumber, normalised to the cylinder's radius. Other notations are as in Fig. 2.

$$\rho_e = \frac{A_e}{V_{Ae}^2}\frac{1}{r}K_1(\lambda r) - \frac{A_e\lambda}{\omega^2 r^2}K_0(\lambda r),$$
$$B_e = \frac{\alpha\mu_0}{B_{0e}}A_e K_1(\lambda r), \quad v_{re} = i\frac{\alpha^2\lambda r}{\rho_{0B}\omega}A_e K_0(\lambda r),$$
$$v_{\phi e} = 0, \quad v_{ze} = \frac{k}{\omega}\frac{\alpha^2 r}{\rho_{0B}}A_e K_1(\lambda r). \tag{17}$$

The amplitudes $A_i$ and $A_e$ are connected with each other by the boundary conditions discussed above, with the use of expressions (10) and (13).

Fig. 5 illustrates the radial structures of the perturbations in the radial direction, giving the snapshots of the radial displacements. The evolution of those displacements in time and along the cylinder could be obtained by multiplying those radial dependences by a harmonic oscillation in time, with the frequency $\omega$, and along the axis of the cylinder, with the wave number $k$. The values of $\omega$ and $k$ are linked with each other by dispersion relation (14).

In the lowest radial harmonic the plasma flows are either always outwards or inwards, depending upon the phase of the oscillation, i.e. either the contraction or rarifaction phase. However, in the higher radial modes, the radial flows change the sign at different radial distances from the axis. This effect is impossible to measure if observing the dynamics of the boundary of the cylinder only, or with imaging telescopes. However, those radial counter-flows should contribute to the non-thermal broadening of emission lines.

## 5. Discussion and conclusions

We have considered linear sausage oscillations of a cold-plasma cylinder embedded in a cold plasma with an azimuthal magnetic field, created by a current on the surface of the cylinder. The magnetic field in the cylinder is parallel to its axis. Such a plasma configuration could be applied to modelling flaring loops, and also magnetic ropes in CME. This equilibrium state is a simplified version of the equilibrium discussed in Mikhalyaev (2005) and KMR12 in the limit of a thick annulus with the azimuthal field. We derived dispersion relations for trapped sausage perturbations, and determined the radial structure of perturbations. This study is the development of the work of KMR12, as, for a simplified model we managed to reproduce the main findings of KMR12, and in addition considered the group speed and higher radial harmonics.

The main feature of the dispersion relation is the existence of a trapped sausage mode in the long-wavelength limit. This result supports the finding of KMR12, and demonstrates that for this effect the presence of the outer region with the field parallel to the axis of the cylinder is not necessary. In the long-wavelength limit the phase speed of the lowest radial harmonic of the sausage mode tends to the external Alfvén speed from below. Thus, according to this model, periods of standing sausage oscillations of coronal loops are determined by the ratio of the loop length to the external Alfvén speed. This estimation is consistent with one made in (Nakariakov et al., 2003). Moreover, of interest is that

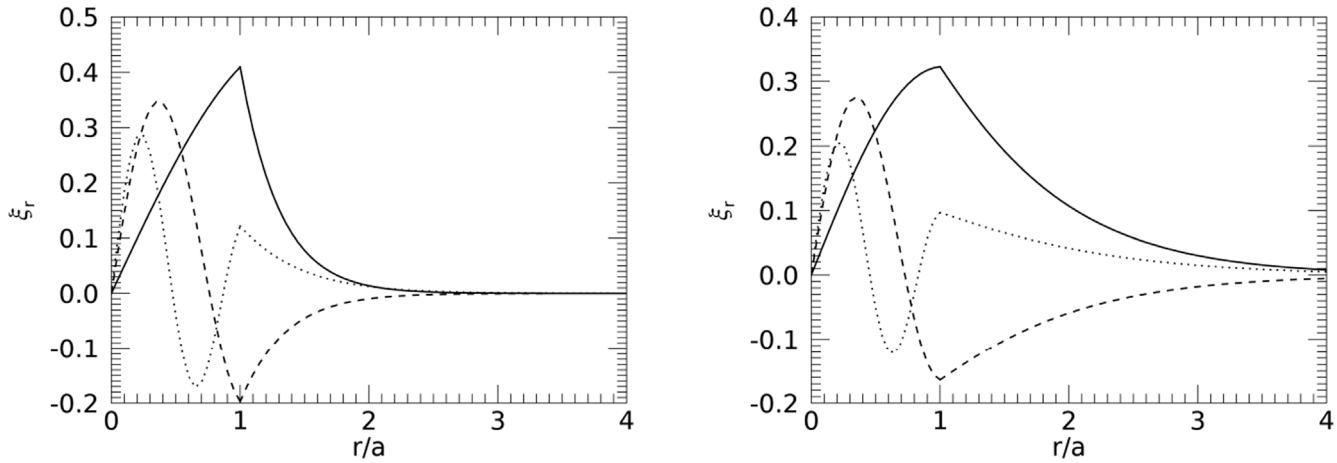


**Fig. 5.** Dependences of the radial displacements on the radial coordinate in the expansion phase of three lowest radial harmonics of the sausage oscillation. Left panel: $V_{Ae}/V_{Ai} = 3$, $ka = 4$; right panel: $V_{Ae}/V_{Ai} = 10$, $ka = 1.5$. The solid, dashed, and dotted curves correspond to the first, second, and third radial harmonics. The displacement is shown in arbitrary units. The radial distance is normalised to the radius of the cylinder.

such a behaviour of the dispersion curve of the fundamental sausage mode is similar to the case of a low-$\beta$ plasma slab with a straight magnetic field, considered by Edwin and Roberts (1982).

Moreover, as pointed out in KMR12, this model could be used for the interpretation of long-period oscillations observed in coronal plasma structures, but usually excluded from the consideration as sausage. Following the discussion in KMR12, consider the 40-s quasi-periodic pulsations of microwave emission in a solar flare, detected by Kupriyanova et al. (2010). In terms of the discussed model, i.e., estimating the phase speed as the ratio of double the flaring loop length of 25 Mm to the oscillation period, we obtain an acceptably realistic value of the external Alfvén speed, 1.25 Mm/s, without the need to assume the existence of the outer region with the parallel field. Interpretation of the 600-s periodicity of the H$\alpha$ intensity variation in a 100 Mm loop, detected by Srivastava et al. (2008), as a sausage mode would require the external Alfvén speed to be 330 km/s. This value is possibly acceptable too, taking into account that it is much higher than the sound speed of the cool plasma filling in the loop. The increase in the period of quasi-periodic pulsations of the thermal emission of a solar flare, from 25 s to 100 s, correlated with the increase in the oscillating loop half-length from 44 Mm to 87 Mm (Dennis et al., 2017), if associated with the sausage oscillation, would require the external Alfvén speed to decrease from 7 Mm/s to 2.9 Mm/s. This range is also consistent with expectations. Likewise, the several-minute periodicities detected by Doyle et al. (2018) in flares on magnetically active dMe stars could be associated with standing sausage oscillations too. The phase relations summarised in Sect. 4 allow one to perform forward modelling of the manifestation of sausage oscillations in different observational bands.

The derived cutoff values of the parallel wave numbers coincide with those values in the case of a cylinder surrounded by a straight field (Roberts et al., 1984) after the substitution of the roots of the zero-order Bessel function $j_{0n}$ instead of $j_{1n}$ in equation (15). The wave number value separating the cutoff values decreases with the increase in the contrast of the external and internal Alfvén speeds, $V_{\mathrm{Ae}}/V_{\mathrm{Ai}}$. Interestingly, the considered density profile in the external medium decreases in the radial direction as $1/r$, which corresponds to the infinite mass in the radial cross-section. However, the higher radial harmonics of the sausage mode are found to have finite cutoffs. This dispersive behaviour is similar to the cases of the uniform external plasma with a parallel magnetic field, considered by KMR12, and the step-function density profile with a straight field everywhere, considered by Edwin and Roberts (1983); Roberts et al. (1984). In both these cases the mass in the radial cross-section is infinite too.

The higher radial harmonics that are characterised by the oscillatory radial structure of the plasma flows inside the cylinder have long wavelengths cutoff, and are leaky for longer wavelengths. The non-monotonic radial structure of the flows in the sausage mode may have important implications for the Zaitsev–Stepanov mechanism for the modulation of the hard X-ray, gamma-ray and microwave emission by sausage oscillations of flaring loops (Zaitsev and Stepanov, 1982). This effect is intrinsic for sausage oscillations of a body kind in a broad range of possible equilibria, and hence is a promising topic for a follow-up study.

The dependence of the group speed of the sausage mode on the parallel wave number has a minimum at a certain value of the wave number. Such a dispersion leads to the formation of the almost monochromatic decay phase of the quasi-periodic fast wave train based on the lowest radial harmonic (e.g. Murawski and Roberts, 1993). The higher radial harmonics could be readily excited if the source, for example a sudden increase in the total pressure inside the cylinder, has a structure significantly different from the radial profile of a certain radial harmonic. For shorter wavelengths those harmonics could contribute to the dispersive formation of a quasi-periodic fast wave train guided by the field-aligned plasma non-uniformity. The specific value of the parallel cutoff wavelength determines the signature of the excited fast wave train and its wavelet spectrum (Nakariakov et al., 2005). In particular, the superposition of several radial harmonics would result in the appearance of short-period “fin”-like features in the wavelet spectra of propagating fast wave trains (e.g. Shestov et al., 2015; Yu et al., 2017). The characteristic periods of the fins are in the vicinity of the cutoff periods described by equation (15). Observational detection of these features together with the use of the estimating expressions for the cutoff wavelengths, i.e. equation (15), would be promising for seismology.

In addition, the results obtained attract attention to the need for accounting for the geometry of the field outside the oscillating plasma structure. In the vast majority of theoretical studies the plasma structure, e.g. a cylinder, is embedded in a plasma with the magnetic field parallel to the cylinder's axis. However, the geometry of a flaring loop is most likely different from the geometry of the background field, for example, in the case of an s-shapped twisted loop. Our results show that even in the simple, analytically treatable case of the azimuthal geometry of the external field, the behaviour of the sausage mode changes significantly. Thus, the effect of a non-parallel external field requires a detailed analysis.

## Acknowledgements

This study was supported by the BK21 plus program through the National Research Foundation funded by the Ministry of Education of Korea. VMN acknowledges the STFC consolidated grant ST/L000733/1.

## References

Bahari, K., 2017. Magnetohydrodynamic sausage waves in current-carrying coronal tubes. Astrophys. Space Sci. 362, 177.
Cally, P.S., 1986. Leaky and non-leaky oscillations in magnetic flux tubes. Sol. Phys. 103, 277–298.
Chen, S.X., Li, B., Kumar, S., Yu, H., Shi, M., 2018. Fast standing modes in transversley nonuniform solar coronal slabs: the effects of a finite plasma beta. Astrophys. J. 855, 47 1801.09204.
Chen, S.X., Li, B., Xia, L.D., Yu, H., 2015a. Periods and damping rates of fast sausage oscillations in multishelled coronal loops. Sol. Phys. 290, 2231–2243 1507.02169.
Chen, S.X., Li, B., Xiong, M., Yu, H., Guo, M.Z., 2015b. Standing sausage modes in non-uniform magnetic tubes: an inversion scheme for inferring flare loop parameters. Astrophys. J. 812, 22 1509.01442.
Chen, S.X., Li, B., Xiong, M., Yu, H., Guo, M.Z., 2016. Fast sausage modes in magnetic tubes with continuous transverse profiles: effects of a finite plasma beta. Astrophys. J. 833, 114 1610.03254.
De Moortel, I., Nakariakov, V.M., 2012. Magnetohydrodynamic waves and coronal seismology: an overview of recent results. Philosophical Trans. R. Soc. Lond. Ser. A 370, 3193–3216 1202.1944.
Dennis, B.R., Tolbert, A.K., Inglis, A., Ireland, J., Wang, T., Holman, G.D., Hayes, L.A., Gallagher, P.T., 2017. Detection and interpretation of long-lived x-ray quasi-periodic pulsations in the x-class solar flare on 2013 may 14. Astrophys. J. 836, 84 1706.03689.
Doyle, J.G., Shetye, J., Antonova, A.E., Kolotkov, D.Y., Srivastava, A.K., Stangalini, M., Gupta, G.R., Avramova, A., Mathioudakis, M., 2018. Stellar flare oscillations: evidence for oscillatory reconnection and evolution of MHD modes. Mon. Not. Roy. Astron. Soc. 475, 2842–2851.
Edwin, P.M., Roberts, B., 1982. Wave propagation in a magnetically structured atmosphere. III - the slab in a magnetic environment. Sol. Phys. 76, 239–259.
Edwin, P.M., Roberts, B., 1983. Wave propagation in a magnetic cylinder. Sol. Phys. 88, 179–191.
Erdélyi, R., Fedun, V., 2007. Linear MHD sausage waves in compressible magnetically twisted flux tubes. Sol. Phys. 246, 101–118.
Gafeira, R., Jafarzadeh, S., Solanki, S.K., Lagg, A., van Noort, M., Barthol, P., Blanco Rodríguez, J., del Toro Iniesta, J.C., Gandorfer, A., Gizon, L., Hirzberger, J., Knölker, M., Orozco Suárez, D., Riethmüller, T.L., Schmidt, W., 2017. Oscillations on width and intensity of slender Ca II H fibrils from sunrise/SuFI. Astrophys. J. Supp. 229, 7 1701.02801.
Giagkiozis, I., Fedun, V., Erdélyi, R., Verth, G., 2015. Axisymmetric modes in magnetic flux tubes with internal and external magnetic twist. Astrophys. J. 810, 53 1706.09669.
Giagkiozis, I., Goossens, M., Verth, G., Fedun, V., Van Doorsselaere, T., 2016. Resonant absorption of axisymmetric modes in twisted magnetic flux tubes. Astrophys. J. 823, 71 1706.09665.
Gruszecki, M., Nakariakov, V.M., Van Doorsselaere, T., 2012. Intensity variations associated with fast sausage modes. Astron. Astrophys. 543, A12.
Guo, M.Z., Chen, S.X., Li, B., Xia, L.D., Yu, H., 2016. Inferring flare loop parameters with measurements of standing sausage modes. Sol. Phys. 291, 877–896 1512.03692.
Hayes, L.A., Gallagher, P.T., Dennis, B.R., Ireland, J., Inglis, A.R., Ryan, D.F., 2016. Quasi-periodic pulsations during the impulsive and decay phases of an x-class flare.

Astrophys. J. Lett. 827, L30 1607.06957.
Inglis, A.R., van Doorsselaere, T., Brady, C.S., Nakariakov, V.M., 2009. Characteristics of magnetoacoustic sausage modes. Astron. Astrophys. 503, 569–575 1303.6301.
Kaneda, K., Misawa, H., Iwai, K., Masuda, S., Tsuchiya, F., Katoh, Y., Obara, T., 2018. Detection of propagating fast sausage waves through detailed analysis of a zebra-pattern fine structure in a solar radio burst. Astrophys. J. Lett. 855, L29.
Khongorova, O.V., Mikhalyaev, B.B., Ruderman, M.S., 2012. Fast sausage waves in current-carrying coronal loops. Sol. Phys. 280, 153–163.
Kopylova, Y.G., Stepanov, A.V., Tsap, Y.T., 2002. Radial oscillations of coronal loops and microwave radiation from solar flares. Astron. Lett. 28, 783–791.
Kupriyanova, E.G., Melnikov, V.F., Nakariakov, V.M., Shibasaki, K., 2010. Types of microwave quasi-periodic pulsations in single flaring loops. Sol. Phys. 267, 329–342.
Kuznetsov, A.A., Van Doorsselaere, T., Reznikova, V.E., 2015. Simulations of gyrosynchrotron microwave emission from an oscillating 3D magnetic loop. Sol. Phys. 290, 1173–1194 1502.06716.
Liu, W., Ofman, L., 2014. Advances in observing various coronal EUV waves in the SDO era and their seismological applications (invited review). Sol. Phys. 289, 3233–3277 1404.0670.
Lopin, I., Nagorny, I., 2014. Fast-sausage oscillations in coronal loops with smooth boundary. Astron. Astrophys. 572, A60.
Lopin, I., Nagorny, I., 2015. Sausage waves in transversely nonuniform monolithic coronal tubes. Astrophys. J. 810, 87.
McLaughlin, J.A., Nakariakov, V.M., Dominique, M., Jelínek, P., Takasao, S., 2018. Modelling quasi-periodic pulsations in solar and stellar flares. Space Sci. Rev. 214, 45 1802.04180.
Melnikov, V.F., Reznikova, V.E., Shibasaki, K., Nakariakov, V.M., 2005. Spatially resolved microwave pulsations of a flare loop. Astron. Astrophys. 439, 727–736.
Mészárosová, H., Rybák, J., Kashapova, L., Gömöry, P., Tokhchukova, S., Myshyakov, I., 2016. Broadband microwave sub-second pulsations in an expanding coronal loop of the 2011 August 10 flare. Astron. Astrophys. 593, A80 1609.04217.
Mikhalyaev, B.B., 2005. Rapid damping of the oscillations of coronal loops with an azimuthal magnetic field. Astron. Lett. 31, 406–413.
Murawski, K., Roberts, B., 1993. Numerical simulations of fast MHD waves in a coronal plasma. II - impulsively generated linear waves. Sol. Phys. 144, 101–112.
Nakariakov, V.M., Foullon, C., Myagkova, I.N., Inglis, A.R., 2010. Quasi-periodic pulsations in the gamma-ray emission of a solar flare. Astrophys. J. Lett. 708, L47–L51.
Nakariakov, V.M., Hornsey, C., Melnikov, V.F., 2012. Sausage oscillations of coronal plasma structures. Astrophys. J. 761, 134.
Nakariakov, V.M., Melnikov, V.F., Reznikova, V.E., 2003. Global sausage modes of coronal loops. Astron. Astrophys. 412, L7–L10.
Nakariakov, V.M., Pascoe, D.J., Arber, T.D., 2005. Short quasi-periodic MHD waves in coronal structures. Space Sci. Rev. 121, 115–125.
Nakariakov, V.M., Pilipenko, V., Heilig, B., Jelínek, P., Karlický, M., Klimushkin, D.Y., Kolotkov, D.Y., Lee, D.H., Nisticò, G., Van Doorsselaere, T., Verth, G., Zimovets, I.V., 2016. Magnetohydrodynamic oscillations in the solar corona and Earth's magnetosphere: towards consolidated understanding. Space Sci. Rev. 200, 75–203.
Roberts, B., Edwin, P.M., Benz, A.O., 1984. On coronal oscillations. Astrophys. J. 279, 857–865.
Shestov, S., Nakariakov, V.M., Kuzin, S., 2015. Fast magnetoacoustic wave trains of sausage symmetry in cylindrical waveguides of the solar corona. Astrophys. J. 814, 135 1510.07908.
Srivastava, A.K., Zaqarashvili, T.V., Uddin, W., Dwivedi, B.N., Kumar, P., 2008. Observation of multiple sausage oscillations in cool post-flare loop. Mon. Not. Roy. Astron. Soc. 388, 1899–1903 0806.0897.
Tian, H., Young, P.R., Reeves, K.K., Wang, T., Antolin, P., Chen, B., He, J., 2016. Global sausage oscillation of solar flare loops detected by the interface region imaging spectrograph. Astrophys. J. Lett. 823, L16 1605.01963.
Van Doorsselaere, T., Kupriyanova, E.G., Yuan, D., 2016. Quasi-periodic pulsations in solar and stellar flares: an overview of recent results (invited review). Sol. Phys. 291, 3143–3164 1609.02689.
Yu, H., Li, B., Chen, S.X., Xiong, M., Guo, M.Z., 2017. Impulsively generated wave trains in coronal structures. I. Effects of transverse structuring on sausage waves in pressureless tubes. Astrophys. J. 836, 1 1612.09479.
Yu, S., Nakariakov, V.M., Selzer, L.A., Tan, B., Yan, Y., 2013. Quasi-periodic wiggles of microwave zebra structures in a solar flare. Astrophys. J. 777, 159 1309.5777.
Yu, S., Nakariakov, V.M., Yan, Y., 2016. Effect of a sausage oscillation on radio zebra-pattern structures in a solar flare. Astrophys. J. 826, 78 1608.04289.
Zaitsev, V.V., Stepanov, A.V., 1982. On the origin of the hard x-ray pulsations during solar flares. Sov. Astron. Lett. 8, 132–134.
Zajtsev, V.V., Stepanov, A.V., 1975. On the origin of pulsations of type IV solar radio emission. Plasma cylinder oscillations (I). Issled. Geomagn. Aeron. i Fiz. Solntsa 37, 3–10.